

Exploring Biodynamic Response (Apparent Masses) of a Seated Human Body Exposed To External Excitation in Vertical Direction

Pratik P. Gaikwad* & Mangesh R. Phate

Pratik P. Gaikwad, Department of Mechanical Engineering, AISSMSCOE, Pune, Maharashtra, India

Mangesh R. Phate, Associate Prof, Department of Mechanical Engineering, AISSMSCOE, Pune, Maharashtra, India

KEYWORDS

Anthropometric data;
Biodynamic model;
Stiffness;
Damping co-efficient;
Apparent mass.

ABSTRACT

The injuries inflicted on a human body are due to the impact of vibrations. In the present work, the biodynamic response behaviors of seated human body subject to vibration in the vertical direction have been extensively examined. The biodynamic response parameter of seated human body has been analyzed in terms of apparent mass (AM). The AM describe “to –the -body” force motion relationship at the interface of human and seat. The present work proposed the six degrees of freedom (6-DOF) analytic biodynamic model of the seated human posture with the backrest in the vertical vibration direction to study the biodynamic response of various masses, stiffnesses, and the damping coefficients. Field test was carried out using a TATA Nanocar to verify the vibrational comfort. The tests were carried out on different surfaces and at different speeds. Acceleration was measured on both seat and head. This paper helps analyze and provide the vibrational comfort to the car driver and the passengers in different road conditions. The present work helps the researchers worldwide to study and analyze the impact of mass, stiffness, and the damping coefficient on the apparent mass.

© 2018 IUST Publication, IJIEPR. Vol. 29, No. 4, All Rights Reserved

1. Introduction

The biodynamic responses of the human body provide us with an understanding of how vibration transmits through the body and, also, contributes to understanding the effects of vibration on comfort, health, and performance. Biodynamic responses are of two types, i.e., “to-the-body” responses and “through-the-body” responses. Driving Point Mechanical Impedance (DPMI) and Apparent Masses (AM) are the “to-

the-body” responses. Seat-to-Head-Transmissibility (STHT) is the “through-the-body” response. The transmission of vibration to the body by seating and other non-rigid structures is dependent on the biodynamic responses of the body. The biodynamic responses of the human body to low-frequency vibration are nonlinear. As explained by Zhou and Griffin (2014), with a transverse excitation of the body, the principal resonance frequency decreases if the magnitude of the vibration excitation increases. This nonlinear softening effect has been found with both random and sinusoidal vibrations.

* Corresponding author: *Pratik P. Gaikwad*

Email: pratik078669@gmail.com

Received 7 August 2018; revised 11 November 2018; accepted 24 December 2018

A. Effects of whole-body vibration:

Various sensations (including satisfaction, anxiety, and ache) are produced when humans are exposed to vibration. In addition, this discomfort interferes with an extensive variety of activities (such as reading and hand control movements). Human body vibration is also the origin of physiological and pathological effects. Low-frequency oscillations of the body cause motion sickness.

B. Causes of disorders:

The environments which may be expected to be related to whole-body vibration injuries are those in which the vibration can be predictable as a source of uneasiness: off-road vehicles (e.g., earth-moving machinery, forest machines, and tractors), road vehicles (e.g., cars, buses, and trucks), helicopters, high-speed marine craft, industrial machinery, and similar environments.

2. Literature Review

Nigam and Malik [2] proposed the use of anthropomorphic models in order to develop a generalized approach to human body vibratory modelling resorting to an experimental program. Gupta T.C [3] considered a 15-degree-of-freedom human model. The base available in this work was the advancement of Nigam and Malik who initiated that an undamped spring mass vibratory model of the human body could be organised through the anthropomorphic model and using the anthropomorphic data and some elastic properties of tissues and bones. The difficulty was to establish damping in the basic spring mass model. Garg and Ross [4] developed the frequency response of standing human subjected to sinusoidal vibration. The vibratory input was the vertical displacement to the feet, and the output was the resulting vertical response of head. They tested twelve subjects (eight males and four females) in the frequency range of 1-50 Hz with small amplitudes. They developed a 16-degree-of-freedom lumped parameter vibratory model.

Chi Liu, Yi Qiu, Michael J. Griffin [5] investigated how forces were circulated over the body-seat interface. Vertical and fore-and-aft forces were measured underneath the ischialtuberosities, middle thighs, and front thighs of 14 subjects sitting on an inflexible flat seat in three postures with a dissimilar thigh contact while exposed to random vertical vibrations at three magnitudes. Xian Xu Bai, Shi Xu Xu, Wei Cheng, Li-Jun Qian [6] projected and

demonstrated a methodology to systematically identify the best configuration or structure of a 4-degree-of-freedom (4DOF) human vibration model and for its parameter identification. An improved version of non-dominated sorting genetic algorithm (NSGA-II) based on Pareto optimization principle was used to determine the model parameters.

N.V. Amar Kishore, A.S. Prashanth, V.H. Saran, and S.P. Harsha [7] explained that the change in the human body mass, pelvic stiffness, and pelvic damping coefficient produced a remarkable change in the biodynamic response behaviors of the seated human body. The influence of a backrest and variation in a seated posture was also studied by Fairley and Griffin [8]. They measured five postures for one subject (slouched, normal, slightly erect, erect, and very erect) and four postures for eight subjects (normal, erect, with backrest, and tense).

An investigation was conducted by Rakheja S. [9] to measure the apparent mass response characteristics of twenty-four human subjects seated in representative automotive postures with hands-in-lap and hands-on-steering-wheel. The measurements were carried out under white noise vertical excitations of 0.25, 0.5, and 1.0 ms⁻² r.m.s. acceleration magnitudes in the 0.5-40 Hz frequency range. Based on the mean value of twenty-four subjects, the apparent mass peak magnitude for subjects seated with hands in their laps was observed in the 6.5-8.6 Hz frequency range with a mean at 7.8 Hz. Mostafa A. M. Abdeen, W. Abbas [10] explained that the developed ANN models presented in their study were very successful in simulating the effect of human body's mass and stiffness on the biodynamic response behaviours under whole-body vibration. They analyzed that the presented ANN models were very efficiently capable of predicting the response behaviors at different masses and stiffnesses rather than those used in the analytic solution.

The study objective of Roberto Deboli, Angela Calvo, Christian Preti [11] was to analyze the dynamic response of an original pneumatic seat installed on old agricultural tractor, when the machine crossed different working surfaces at different tire pressure degrees at different forward speeds and with or without ballast and implement.

Based on the analysis and validation, Cho-Chung Liang et al. [12] concluded that the lumped-parameter models were limited to one-dimensional analysis. Therefore, the human body

in this study was considered to be sitting erect without backrest support irrespective of hands' position, while feet were supported and vibrated. These mathematical models included linear and nonlinear systems with varying degrees of complexity depending on the analysis objective. The solution technique used for linear models is called FD method, and that for nonlinear ones is termed TD method.

The FD method takes the Fourier transformation of the system EQMs to obtain the steady-state response of the system. On the other hand, the TD method utilizes the fourth-order Runge-Kutta method to receive the time history of the system, including transient and steady-state responses. To be consistent, only steady-state response is selected in the evaluation of the above three biodynamic response functions. According to the simulations of all lumped-parameter models listed in the study, the one developed by Wan and Schimmels (1995) matched experimental data most closely.

James L. Coyte, David Stirling [13] conducted a survey of Whole Body Vibration research, and concluded that there was a clear consent in industrial security and epidemiology research where the relation between vibration dosage and lower back pain (LBP) was difficult to determine due to the additional variables including age, posture, and uncertainties. Because of current developments in MEMS technology, MIMO system frequency response estimation in 5-DOF has become increasingly more sensible to implement, even though it remains very difficult to analyze due to the complexities of cross-coupled motion.

A wide variety of approaches were employed to design biodynamic models. In the application of control systems, because it is desirable for the body model to be robust, the main problems which have not been solved yet include model over-fitting and the identification of body model parameters in real time. The existing research in control systems has modelled the human body mass with uncertain parameters and has achieved robust performance. There is a lack of research investigating the performance of active seating suspension control systems under the intersubject and intrasubject variations.

Comprehensive seated WBV analysis has been undertaken with both optical and inertial motion capture systems. Both systems have their respective advantages and disadvantages. Inertial motion sensors have the potential to replace optical motion capture systems with further

developments in software and MEMS technologies.

Neil J. Mansfield [14] explained that the exposure to whole-body vibration was a risk factor in the development of low back pain. In order to develop a full understanding of the response of the seated person to vibration, they conducted experiments in the laboratory investigating the biomechanics of the seated person. Some of their methods are based on the driving force and acceleration at the seat and are reported in their literature as apparent mass, driving point mechanical impedance or absorbed power.

Their paper introduced the background behind such impedance methods, the theory, and application of the methods. It presented example data showing typical responses of the seated human to whole-body vibration in the vertical, fore-and-aft, and lateral directions. In addition, it highlighted problems that researchers might encounter in performing, analyzing, and interpreting human impedance data.

Rasul Jamshidi [15] presented a new arithmetical model to optimize the arrangement policy for machines and human resources. He explained that fatigue-recovery and learning-forgetting processes are important factors in human resource scheduling, and the core factor in machines maintenance is reliability.

He pooled the concept of reliability, fatigue-recovery, and learning, not recalling for a broad study of human-machine systems, as a separate research of human resources scheduling, and machines scheduling is not steady with the definite situation of human-machine systems. The results indicated that the model could obtain resourceful and helpful work-rest schedule and maintenance schedule.

Esmail Mehdizadeh and Amir Fatehi-kivi [16] projected an arithmetical model into the single-item capacitated lot-sizing problem with backlogging, protection stocks, restricted outsourcing with dissimilar production methods, limited storehouse space, and fuzzy parameters. Authors utilized a possibility approach to convert the fuzzy single item capacitated lot-sizing model to an equivalent crisp single-item capacitated lot-sizing model.

Due to the complication of the problem, a vibration damping optimization (VDO) algorithm was utilized to resolve the problem. Their experimental results showed that the vibration damping optimization (VDO) algorithm enhanced performance than other two presented

algorithms for solving this model, especially for large-sized problems.

Hassan Sadeghi Naeini, Koustuv Dalal, Seyed Hashem Mosaddad and Karmegam Karuppiyah [17] conducted a review of Economic Effectiveness of Ergonomics Interventions. This review highlighted two methods to illustrate the economic effectiveness of ergonomics.

One of them was the need for publishing papers, which included valid economics model about industrial ergonomics. In this view, creating a suitable interaction between ergonomist and economics specialists is essential. The second method concerns the shortage of documents about the economic benefits of ergonomic products design. As a result, the interaction between occupational ergonomics experts, economics authorities, and product designers within the industrial sectors should be considered.

Aaron M. Kociolek, Angelica E. Lang, Catherine M. Trask [18] concluded that fieldwork exploration of rural workers using quad bikes demonstrated a strong relationship between simultaneously recorded vertical accelerations at the seat and head. Spectral analysis of Z-axis seat and head vibration revealed strong coherence between 1.3 and 4.9 Hz with an amplified and out-of-phase vertical vibration at the head/neck relative to the seat in that frequency range. While their results are indicative of spinal resonance in the vertical direction, the absence of published thresholds for the cervical spine means that it is unknown whether the current exposure can lead to neck pain, previously observed in rural workers who use quad bikes.

Other factors, such as mechanical shocks and sustained postures, and non-vibration factors, such as handling manual materials, may also play some part in musculoskeletal disorders of the neck in the farming community. These amplified and out-of-phase vibrations measured at the head relative to the pelvis, in this sample of rural workers using quad bikes, became a focus for future laboratory-based investigation to determine biodynamic, proprioceptive, and perceptual effects of such exposures.

The developed 6-DOF biodynamic model is, as shown in "Fig.1."

3. Biomedical 6-DOF Model

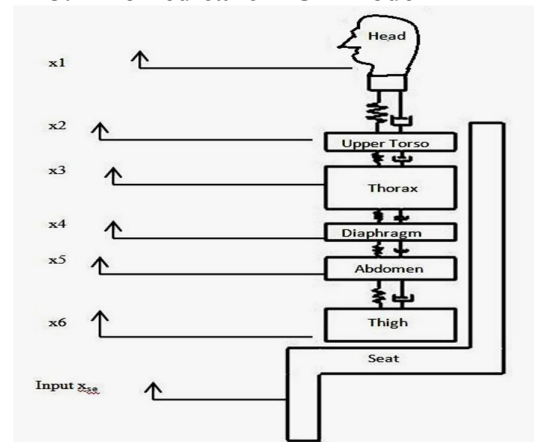


Fig. 1. Developed Model of 6-DOF

Equations of motion:

The equation of motion of the human body can be obtained as follows:

$$m_1 \ddot{x}_1 = -c_1 (\dot{x}_1 - \dot{x}_2) - k_1 (x_1 - x_2),$$

$$m_2 \ddot{x}_2 = c_1 (\dot{x}_1 - \dot{x}_2) + k_1 (x_1 - x_2) - c_2 (\dot{x}_2 - \dot{x}_3) - k_2 (x_2 - x_3),$$

$$m_3 \ddot{x}_3 = c_2 (\dot{x}_2 - \dot{x}_3) + k_2 (x_2 - x_3) - c_3 (\dot{x}_3 - \dot{x}_4) - k_3 (x_3 - x_4),$$

$$m_4 \ddot{x}_4 = c_3 (\dot{x}_3 - \dot{x}_4) + k_3 (x_3 - x_4) - c_4 (\dot{x}_4 - \dot{x}_5) - k_4 (x_4 - x_5),$$

$$m_5 \ddot{x}_5 = c_4 (\dot{x}_4 - \dot{x}_5) + k_4 (x_4 - x_5) - c_5 (\dot{x}_5 - \dot{x}_6) - k_5 (x_5 - x_6)$$

$$m_6 \ddot{x}_6 = c_5 (\dot{x}_5 - \dot{x}_6) + k_5 (x_5 - x_6) - c_6 (\dot{x}_6 - \dot{x}_{se}) - k_6 (x_6 - x_{se}).$$

This equation of motion can be expressed in the matrix form as given by "Eq.(1)"

$$[M]\{\ddot{x}\} + [C]\{\dot{x}\} + [K]\{x\} = \{f\} \quad (1)$$

where [M], [K], and [C] are mass, stiffness, and damping matrices, respectively. {f} is the force vector due to external excitation. M, K, C and excitation force matrix are calculated by the following "Eq. (2a-2d)"

$$[M] = \begin{bmatrix} m_1 & 0 & 0 & 0 & 0 & 0 \\ 0 & m_2 & 0 & 0 & 0 & 0 \\ 0 & 0 & m_3 & 0 & 0 & 0 \\ 0 & 0 & 0 & m_4 & 0 & 0 \\ 0 & 0 & 0 & 0 & m_5 & 0 \\ 0 & 0 & 0 & 0 & 0 & m_6 \end{bmatrix} \quad (2a)$$

$$[C] = \begin{bmatrix} c_1 & -c_1 & 0 & 0 & 0 & 0 \\ -c_1 & c_1 + c_2 & -c_2 & 0 & 0 & 0 \\ 0 & -c_2 & c_2 + c_3 & -c_3 & 0 & 0 \\ 0 & 0 & -c_3 & c_3 + c_4 & -c_4 & 0 \\ 0 & 0 & 0 & -c_4 & c_4 + c_5 & -c_5 \\ 0 & 0 & 0 & 0 & -c_5 & c_5 + c_6 \end{bmatrix} \quad (2b)$$

$$[K] = \begin{bmatrix} k_1 & -k_1 & 0 & 0 & 0 & 0 \\ -k_1 & k_1 + k_2 & -k_2 & 0 & 0 & 0 \\ 0 & -k_2 & k_2 + k_3 & -k_3 & 0 & 0 \\ 0 & 0 & -k_3 & k_3 + k_4 & -k_4 & 0 \\ 0 & 0 & 0 & -k_4 & k_4 + k_5 & -k_5 \\ 0 & 0 & 0 & 0 & k_5 & k_5 + k_6 \end{bmatrix} \quad (2c)$$

$$\{f\} = \begin{Bmatrix} 0 \\ 0 \\ 0 \\ 0 \\ 0 \\ C_6 \dot{X}_{se} + K_6 X_{se} \end{Bmatrix} \quad (2d)$$

The Fourier Transformation of “Eq. (1)” is given by the “Eq. (3)”

$$(-\omega^2 M + j\omega C + K) \cdot Z(j\omega) = F_z(j\omega) \quad (3)$$

where $j = (\sqrt{-1})$ is the complex phasor, and ω is the angular frequency. The solution can be obtained as given by “Eq. (4a-4b)”.

$$Z(j\omega) = [Z1(j\omega), Z2(j\omega), Z3(j\omega), Z4(j\omega)]^T \quad (4a)$$

$$F_z(j\omega) = [0, 0, 0, (K_4 + j\omega C_4)Z_0(\omega) = \begin{bmatrix} 0 & 0 \\ 0 & 0 \\ 0 & 0 \\ 0 & 0 \\ 0 & 0 \\ K_6 & C_6 \end{bmatrix} \begin{bmatrix} 1 \\ j\omega \end{bmatrix} Z_0(j\omega) \quad (4b)$$

Combining Eqs. (3) and (4), $Z(j\omega)$ can be rewritten as “Eq. (5)”:

$$Z(j\omega) = A^{-1} B \begin{bmatrix} 1 \\ j\omega \end{bmatrix} Z_0(j\omega) \quad (5)$$

$$\text{with } A = -\omega^2 M + j\omega C + K \quad (6a)$$

$$B = \begin{Bmatrix} 0 & 0 \\ 0 & 0 \\ 0 & 0 \\ 0 & 0 \\ 0 & 0 \\ K_6 & C_6 \end{Bmatrix} \quad (6b)$$

Based on Eqs. (5) and (6), the correlation between dynamic response $Z(j\omega)$ and excitation $Z_0(\omega)$ of the masses can be calculated.

4. Biodynamic Response Parameters

Biodynamic Responses help us understand that how human body responses to vibration vary with the frequency and direction of vibration.

Newton’s second law of motion states that “the rate of change of momentum of a body is proportional to the force acting on it and is in the direction of the force” and can be summarized by “Eq. (7)”:

$$\text{Force} = \text{mass} * \text{Acceleration} \quad (7)$$

where m is the mass. For a rigid mass, this equation holds at all frequencies. However, for a non-rigid system, such as the body of human, the force necessary for accelerating the supporting surface is a composite function of frequency. This function is available in terms of the ‘apparent mass’ equated in “Eq. (8)” as follows:

$$M(\omega) = \frac{F(\omega)}{a(\omega)} \quad (8)$$

where $M(\omega)$ is the apparent mass at frequency ω . The units of apparent mass are in kg. The apparent mass of an inflexible mass is not a function of frequency, yet is equivalent to its static mass. For human subjects, this means that the apparent mass is barely a function of their dynamic characteristics but also of their supported weight. This can make it complex to relate the data between subjects of different weights. The apparent mass modulus should tend towards an origin that is equivalent to the supported weight, and the segment should have an origin of 0° . Apparent Mass (AM) is defined as the ratio of functional periodic excitation force to the resulting vibration acceleration at the same frequency [6] and is expressed in “Eq. (9)” as follows:

$$AM = \frac{K_6 + (j\omega)C_6}{-\omega^2} [1 - [1, 0, 0, 0, 0, 0]A^{-1} B] \begin{bmatrix} 1 \\ j\omega \end{bmatrix} \quad (9)$$

5. Experimentation

Experimentation was performed at AISSSMS College of Engineering Pune. Smooth and Rough road surfaces were selected. Experimentation was performed on four males and two females. To obtain the frequency ranges is the aim of experimentation.

Tab. 1. Levels Selected for the Experimentation

S. No.	Parameters	Levels	
1	Parameter 1 (Weight)	1 (Low) 35-55 kg	2 (High) 56-85 kg
2	Parameter 2 (Speed)	0-20 kmph	20-40 kmph
3	Parameter 3 (Road Surface)	Smooth	Rough
4	Parameter 4 (Gender)	Male	Female

Tab. 2. Anthropometric Measurements for 6DOF model of 6 Subjects[1]

S.No.	Dimensional	Measurements (cm)					
		Male1	Male2	Male3	Male4	Female1	Female2
L1	Standing height	175	168.8	170.5	176	160	158
L2	Shoulder height	148	138.6	143.7	149.5	134	133.5
L3	Armpit height	138.8	136.8	138	139.6	135.5	135
L4	Waist height	109.8	107.7	109	110.5	106.2	105.6
L5	Seated height	94.8	92.2	94	96.2	91.5	91.1
L6	Head length	19	20.5	18.4	19.2	16.4	16.8
L7	Head breadth	21.5	20.5	21	20.2	18.8	19.2
L8	Head to chin height	20.5	21.2	20.2	20.5	16.5	17
L9	Neck circumference	38.5	37.2	37.9	38.9	36.95	35.95
L10	Shoulder breadth	44.2	43.6	43.2	44.8	42.3	41.2
L11	Chest depth	26.3	22.2	23.3	22.3	26.8	26.8
L12	Torso Height	12.3	11.6	11.5	13	13.5	13.5
L13	Torso breadth	44.8	43.5	41.5	42.8	40.5	42.5
L14	Torso depth	18.5	18.5	18	18.2	18.8	19.4
L15	Torso circumference	52.5	51.8	50	51.9	48.9	48.5
L16	Thorax Height	22.5	18.8	22.5	21.5	22	21
L17	Thorax Breadth	33.5	32.8	31.2	33.2	30.5	30
L18	Thorax Depth	18	20	17.5	17.4	21.5	22.5
L19	Thorax circumference	51.5	50.8	50	51.8	48.5	48.6
L20	Diaphragm Height	9.6	8.5	8.5	8.5	7.5	7.5
L21	Diaphragm Breadth	22.3	22	21.3	21.3	20	18
L22	Diaphragm Depth	14	14	14.5	14.2	14	14
L23	Diaphragm Circumference	41.5	41.2	40	41.9	39.4	39
L24	Abdomen Height	20.4	20.5	21.2	20.2	18.4	17.5
L25	Abdomen Breadth	39.4	39.5	39	38.5	38.5	37.8
L26	Abdomen Depth	26.4	25	27.2	26.5	24.5	24.5
L27	Thigh Circumference	38.8	38	38	36.5	35.5	35.5
L28	Shoulder to Elbow length	33.5	31.5	32.5	33.5	30.5	30.5
L29	Knee Height Seated	54.5	50.4	52.8	53.5	51	49
	Weight	83.5 kg	67.2 kg	70.4kg	63 kg	49.5 kg	51.6 kg

5-1. Input / output parameters

Based on the literature review and previous works done among many independently controllable parameters affecting biodynamic

response of seated human model, the parameters viz., Weight (A), Speed (B), Road Profile(C), Gender (D) and two levels of low and high, were

selected as primary parameters for the study. Table 1 shows the parameters used for the experimentation. Experimental setup is as shown in “Fig. 2”. Car at a speed of 0-20 kmph and 20-40 kmph was driven for a range of 15 metres with the accelerometers mounted on one at base/seat of subject and another mounted at the head of subjects. Triaxial accelerometers were used with four-channel Fast Fourier transform (FFT) analyzer. Experiment was performed on four males and two females. Weights of these subjects were in the range of 40-80 kg.



Fig. 2. Experimentation Setup

Table 2 shows the anthropometric measurements of four-male and two-female subjects used for experimentation. These measurements were used for the calculation of Mass, Stiffness, and Damping Co-efficient of human body segments.

5-2. Observation

Tab. 3. Observations taken during experimentation

S.No.	Sample 1 Experimental	Speed kmph	Acc ⁿ . mm/s ²	Freq. Hz
1	a Smooth Head	0-20	90	6
	b Smooth Seat	0-20	56.3	7
	c Transmissibility Ratio(TR)		1.5985	
2	a Smooth Head	20-40	192.7	5
	b Smooth Seat	20-40	57.2	5
	c Transmissibility Ratio(TR)		3.368	
3	a Rough Head	0-20	149.8	6
	b Rough Seat	0-20	36.49	5
	c Transmissibility Ratio(TR)		4.105	
4	a Rough Head	20-40	379.9	5
	b Rough Seat	20-40	64.6	6
	c Transmissibility Ratio(TR)		5.880	

Results were obtained by the NVGate Oros software with Fast Fourier Transform (FFT) analyzer. Table 3 shows the observations of the results. According to the observations, it is seen that peak accelerations are obtained within the range of 0-20 Hz frequency. Thus, analytical calculations are done.

6. Calculation of Mass, Stiffness, and Damping Coefficient Matrix

Calculation of Mass, Stiffness, and Damping Co-efficient is required to obtain the biodynamic responses of each individual.

6-1. Mass matrix calculation for 6DOF

On the basis of Anthropometric data [1], the proportion of the total body weight estimated for different body segments is:

- (Head + Neck) $M_1 = 7.5$ % of Total Body Mass
- Upper Torso $M_2 = 4.21$ % of Total Body Mass
- Thorax $M_3 = 21.516$ % of Total Body Mass
- Diaphragm $M_4 = 3.11$ % of Total Body Mass
- Abdomen $M_5 = 23.776$ % of Total Body Mass
- Thigh $M_6 = 18.2$ % of Total Body Mass

Mass
Based on the above formulae, Division of Masses of 6 subjects for 6 degrees of freedom was

calculated. These distributions of masses into segments are shown in Table 4.

Tab. 4. Mass distribution by segments of four males and two females

	Male 1 (83.5 kg)	Male 2 (67.2 kg)	Male3 (70.4kg)	Male4 (63kg)	Female1 (49.5kg)	Female2 (51.6kg)
M ₁	6.26	M ₁ 5.04	M ₁ 5.28	M ₁ 4.72	M ₁ 3.71	M ₁ 3.87
M ₂	3.51	M ₂ 2.82	M ₂ 2.96	M ₂ 2.65	M ₂ 2.08	M ₂ 2.17
M ₃	18.80	M ₃ 15.1	M ₃ 15.8	M ₃ 14.1	M ₃ 11.1	M ₃ 11.6
M ₄	2.58	M ₄ 2.08	M ₄ 2.18	M ₄ 1.95	M ₄ 1.53	M ₄ 1.59
M ₅	19.8	M ₅ 15.9	M ₅ 16.7	M ₅ 14.9	M ₅ 11.7	M ₅ 12.2
M ₆	15.19	M ₆ 12.2	M ₆ 12.8	M ₆ 11.4	M ₆ 9.09	M ₆ 9.39

6-2. Stiffness matrix calculation for 6DOF

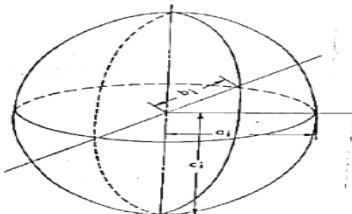


Fig. 3. Semi Ellipsoid [3]

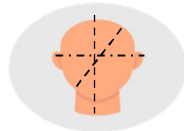


Fig. 4. Human Head segment [3] Axes

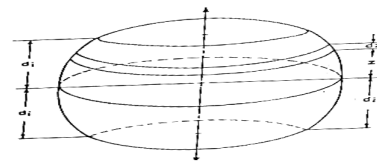


Fig. 5. Truncated ellipsoid [3]

For evaluating the stiffness of the segment, the axial tension of a truncated ellipsoid is considered as shown in “Figs.3 and 5”. In the field of the assumptions regarding the mechanical properties and neglecting the strains due to the self-weight in comparison to those caused by the forces a body may have to withstand, the expression of axial stiffness S_i of the ellipsoid may be derived, as shown in “Eq. (10)” as follows:

$$S_i = (\pi E a_i b_i) / (c_i I_i), \text{ kN/m} \tag{10}$$

Tab. 5. Calculation of Semi Ellipsoid axes [4]

Body Segment	Mass Element (kg)	Formulae		
		a _i	b _i	c _i
Head+ Neck	M ₁	(L7/2)+(L8/2π)	(L7/2)+(L8/2π)	(L6/2)+((L1-L2-L6)/2)
Upper Torso	M ₂	(L13/2)	(L14/2)	(L12/2)
Thorax	M ₃	(L17/2)	(L18/2)	(L16/2)
Diaphragm	M ₄	(L21/2)	(L22/2)	(L20/2)
Abdomen	M ₅	(L25/2)	(L26/2)	(L24/2)
Thigh	M ₆	(L27/2π)	(L27/2π)	((L2-L28-L29)/2)

Where,
 $E = (E_b * E_t)^{1/2}$ (11)
 E = Modulus of Elasticity of Human Body (13.06 MN/m²)
 E_b = Elastic Modulus of Bone (22.6 GN/m²)
 E_t = Elastic Modulus of Tissue (7.5 kN/m²)
 d_i is the half length of the truncated ellipsoid.

The Moment of inertia of each ellipsoid segment can be calculated by using “Eq. (12)”.

$$I_i = \log ((2\text{-tr}^2)/\text{tr}^2) \quad (12)$$

where

$\text{tr}^2 = 1 - d_i/c_i$ may be referred to as the truncation factor.

d_i is the half length of the truncated ellipsoid.

The same ellipsoidal segment has been used by Nigam and Malik in their vibratory model and truncation of 5% at both ends, i.e., $d_i = 0.95 c_i$. In this work, the same truncation factor is assumed; therefore, the segmental stiffness can be expressed as follows:

$$S_i = (0.857524 * E a_i b_i) / c_i, \text{ kN/m}$$

Substituting value of $E = 13.06 \text{ MN/m}^2$,

$$S_i = (11164.277 a_i b_i) / c_i, \text{ kN/m} \quad (13)$$

By using Eq. (13), segmental stiffness is calculated, and stiffness of spring element (K_i) is calculated as shown in Table 6.

Tab. 6. Stiffness Calculation [3]

Sr. No.	Stiffness of Spring Element (kN/m)	Formulae
1	K_1	S_1
2	K_2	$S_2 S_3 / (S_2 + S_3)$
3	K_3	$S_3 S_4 / (S_3 + S_4)$
4	K_4	$S_4 S_5 / (S_4 + S_5)$
5	K_5	$S_5 S_6 / (S_5 + S_6)$
6	K_6	S_6

Table 7 shows the stiffness in N/m for four males and two females of six segments.

Tab. 7. Stiffness distribution by segments of Four males and Two females

Male 1 (83.5 kg)	Male 2 (67.2 kg)	Male 3 (70.4 kg)	Male 4 (63 kg)
K_1 2630 02	K_1 1370 00	K_1 1570 00	K_1 1500 00
K_2 1070 00	K_2 1300 00	K_2 9860 0	K_2 1040 00
K_3 8200 0	K_3 9920 0	K_3 8120 0	K_3 8550 0
K_4 1110 00	K_4 1150 00	K_4 1180 00	K_4 1170 00
K_5 1310 0	K_5 1370 0	K_5 1330 0	K_5 1600 0
K_6 1370 0	K_6 1440 0	K_6 1400 0	K_6 1210 0

Tab. 7. Continue

Female1 (49.5 kg)		Female2 (51.6 kg)	
K_1	124000	K_1	138000
K_2	109000	K_2	118000
K_3	92500	K_3	91700
K_4	121000	K_4	115000
K_5	13000	K_5	12600
K_6	13600	K_6	13200

6-3. Damping coefficient mass for 6DOF

Damping of the Vibratory Model:

Tab. 8. Standard Damping Ratio [4]

S. No.	Body Segment	Damping constant, ξ_i
1	Head and Neck	0.009445
2	Upper Torso	0.3212
3	Thorax	0.0868
4	Diaphragm	0.3809
5	Abdomen	0.675
6	Thighs	0.5

Table 8 shows the Damping constant, ξ_i , for six segments of human body. Values of ξ_i are taken from standards [4].

By obtaining Damping constants, ξ_i , the damping ratio can be calculated, as shown in Eq. (14).

The damping ratio of the i^{th} segment is given by

$$\beta_i = \xi_i * (S_i M_i)^{1/2} \quad (14)$$

where

ξ_i = Damping constant of the i^{th} segment (N-s/m)

β_i = Damping ratio of the i^{th} segment

S_i = Stiffness of the segment (kN/m)

M_i = Mass of the segment, kg.

Tab. 9. Damping co-efficient [3]

Sr. No.	Damping element Designation- sec/m	Formulae
1	C_1	$2\beta_1 \beta_2 / (\beta_1 + \beta_2)$
2	C_2	$2\beta_2 \beta_3 / (\beta_2 + \beta_3)$
3	C_3	$2\beta_3 \beta_4 / (\beta_3 + \beta_4)$
4	C_4	$2\beta_4 \beta_5 / (\beta_4 + \beta_5)$
5	C_5	$2\beta_5 \beta_6 / (\beta_5 + \beta_6)$
6	C_6	$2\beta_6$

Table 9 shows the calculation of damping co-efficients in N-sec/m. In Table 10, these damping co-efficients are calculated for six segments of human body for four males and two females.

Tab. 10. Damping element distribution by segments of four males and two females

Male 1 (83.5kg)		Male 2 (67.2kg)		Male3 (70.4 kg)		Male4 (63 kg)	
C ₁	2030000	C ₁	12800	C ₁	15300	C ₁	13100
C ₂	310000	C ₂	296000	C ₂	242000	C ₂	224000
C ₃	207000	C ₃	197000	C ₃	177000	C ₃	164000
C ₄	342000	C ₄	304000	C ₄	320000	C ₄	281000
C ₅	272000	C ₅	228000	C ₅	233000	C ₅	181000
C ₆	282000	C ₆	238000	C ₆	242000	C ₆	187000

Tab. 10. Continue

Female1 (49.5 kg)		Female2 (51.6)	
C ₁	8530	C ₁	9880
C ₂	183000	C ₂	206000
C ₃	139000	C ₃	140000
C ₄	231000	C ₄	218000
C ₅	159000	C ₅	162000
C ₆	165000	C ₆	167000

7. Result and Discussion

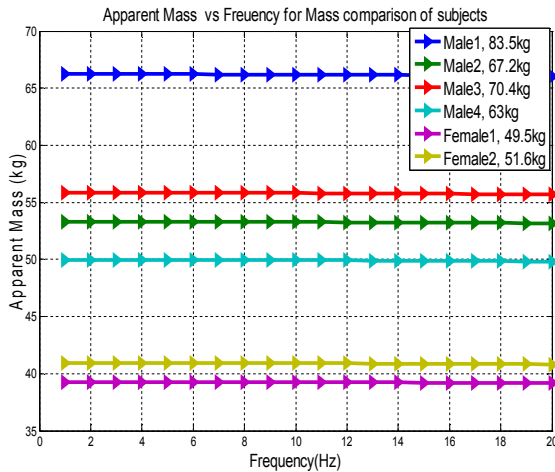


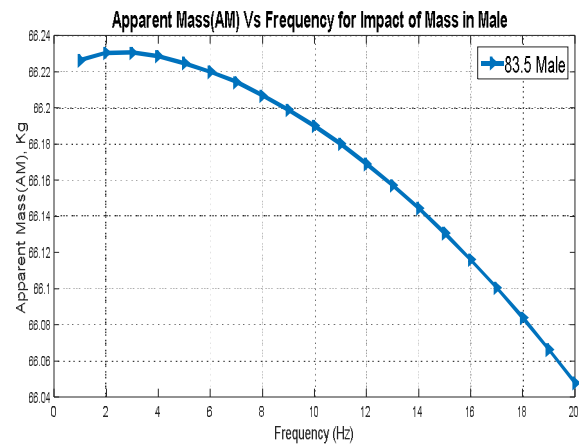
Fig. 6. Effect of Human Body’s Mass on the Biodynamic Response behaviour (AM) for varying Weights of Male and Female (Analytical)

Fig. 6 shows the plot of Apparent Masses (AM) vs. Frequency of 4 males and 2 females varying according to their weights. Based on Fig. 6, Apparent Masses (AM) are higher in the case of a person with higher weights.

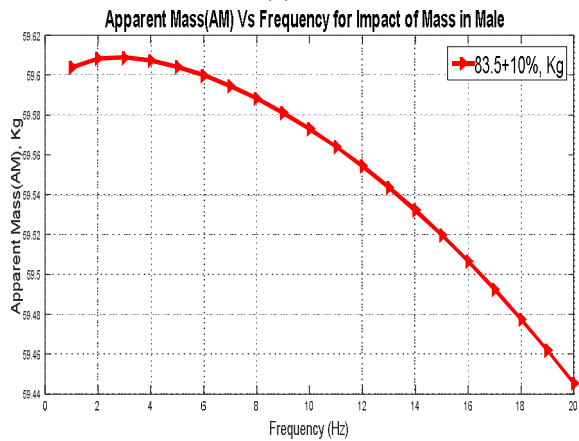
Based on Figs. 7 (a)–7(d), it is observed that the impact of mass is significant on AM. The response AM continues increasing w.r.t an increase in the weight. Both of the responses are

increasing w.r.t the frequency for the initial frequency range of 1-5 Hz and, then, go on decreasing after the peak level. Increasing the body by 10% in both male and female passengers

leads to a decrease in primary resonance frequency and remarkably higher peak biodynamic responses.



(a)



(b)

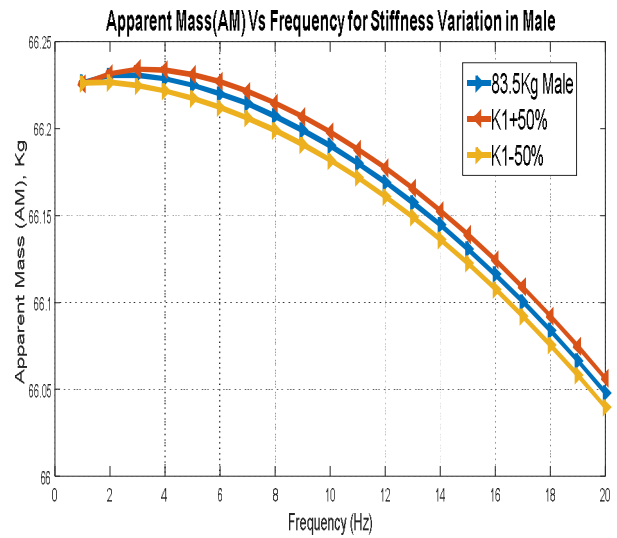
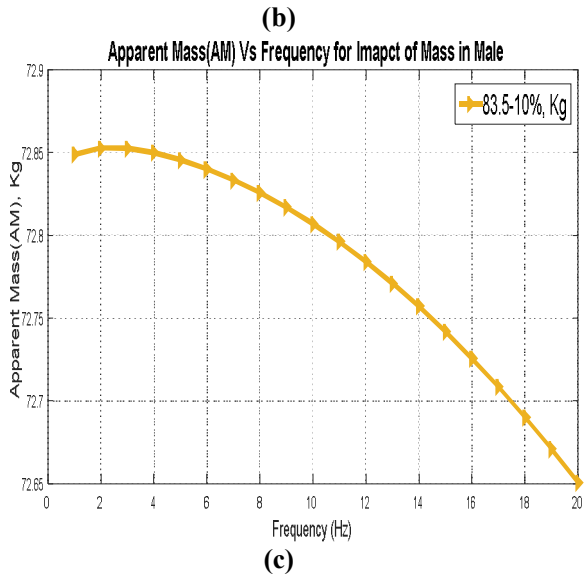


Fig. 8. Effect of Stiffness co-efficient on the Biodynamic Response behaviour (AM) on Male1 (Analytical)

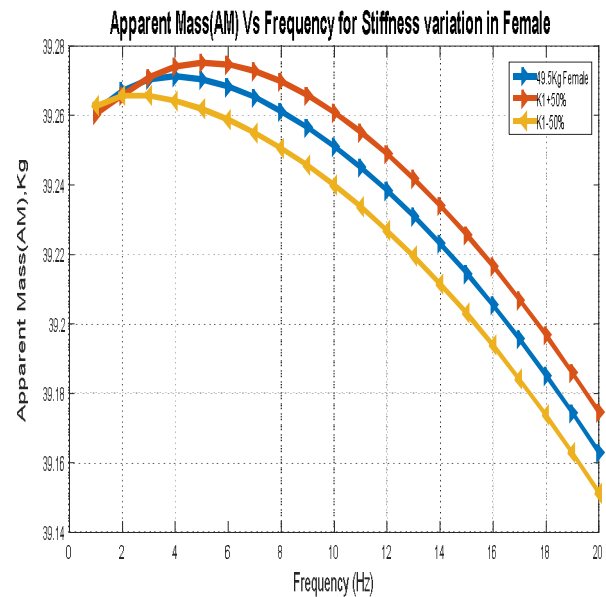
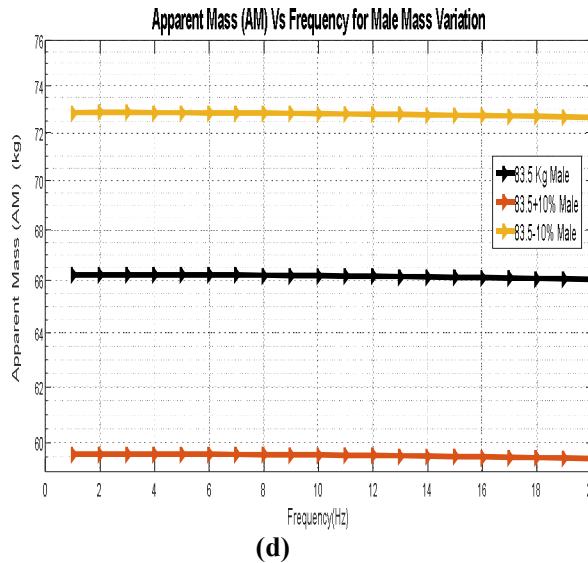


Fig. 9. Effect of Stiffness co-efficient on the Biodynamic Response behaviour (AM) on Female1 (Analytical)

Fig. 7a-d. Effect of Mass Variation of Human Body (male) on the Apparent Mass (AM)

* Note: The comparative graph is given only to show the impact of the mass. The actual nature of the graph is not a straight line; the variation of response AM w.r.t frequency is shown in Figs.7a & 7c. Accordingly, it is clear that Apparent Masses (AM) increase with an increase in Mass.

Three distinct values of neck stiffness K_1 for normal K_1 , $K_1+50\%$, and $K_1-50\%$ are used to examine the effect of Neck Stiffness on the response behaviors of human body, as shown in Figs. 8 and 9. Based on Figs. 8 and 9, it is clear that by increasing the neck stiffness, the biodynamic response characteristics of seated human body, i.e., Apparent Masses (AM), are increased; by decreasing the neck stiffness, the biodynamic response characteristics, i.e., Apparent Masses (AM), are decreased.

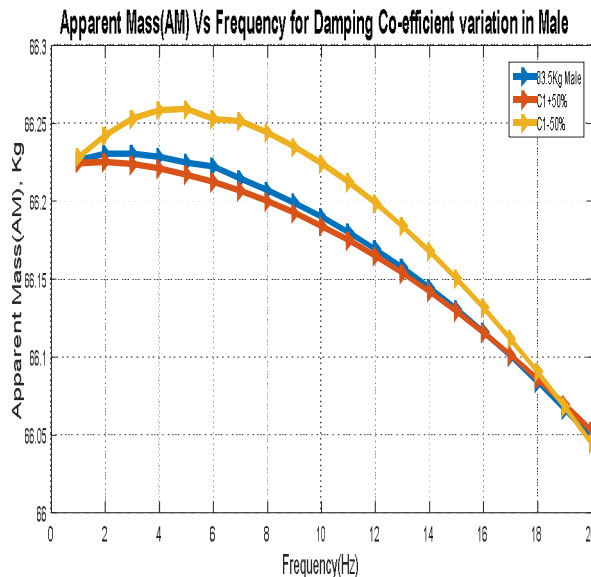


Fig. 10. Effect of Damping co-efficient on the Biodynamic Response behaviour (AM) on Male 1 (Analytical)

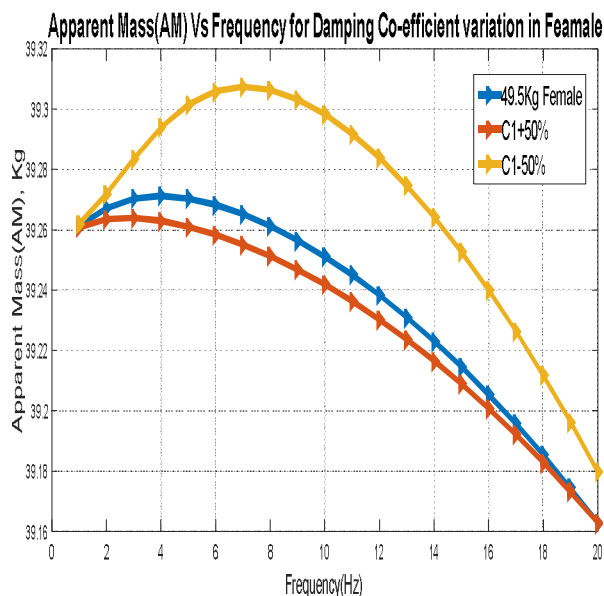


Fig. 11. Effect of Damping co-efficient on the Biodynamic Response behaviour (AM) on Female 1 (Analytical)

Three distinct values of neck stiffness C_1 for normal C_1 , $C_1+50\%$, and $C_1-50\%$ are used to examine the effect of Neck Stiffness on the response behaviors of human body, as shown in "Figs. 10 and 11".

According to Figs. 10 and 11, it is clear that by increasing the neck damping co-efficient, the biodynamic response characteristics of seated human body, i.e., Apparent Masses (AM), are

decreased; by decreasing the neck damping co-efficient, the biodynamic response characteristics, i.e., Apparent Masses (AM), are increased.

8. Conclusion

The main objective of the present work was to analyze the biodynamic response, i.e., apparent mass (AM), for the seated human body in the car, when the car is moving at different speeds and on different road surfaces. Analytical studies conducted on the human body give us the conclusion that the whole body vibration can cause neck injury, resulting in chronic neck pain. The human body is an enormously complex-active multi-body dynamic system, the properties of which differ with time. Thus, to analyze and find procedures and methods to decrease the effects of vibration on the human body based on such a model is the most important objective. The biodynamic responses of seated human operators are distinguished and useful in designing and improving the anti-vibration devices and/or test dummies; it is of immense significance and engineering significance to institute simple and effective biodynamic models of seated occupants. Based on the analytical results, it could be concluded that the change in human body's mass, neck stiffness, and neck damping coefficient produced a notable change in biodynamic response behaviors of seated human body. Thus, it can be concluded that the biodynamic response characteristic, i.e., Apparent Masses (AM), directly corresponds to human body's mass and neck stiffness coefficient and inversely corresponds to neck damping coefficient.

References

- [1] Chakarbarti, D., "Indian Anthropometric Dimensions for Ergonomic Design Practice," 1st ed., National Institute of Design, (1997), PP. 15-99.
- [2] Nigam, S.P., Malik, M., "A study on a vibratory model of a human body", Journal of Biomechanical Engineering, Vol. 109, No. 2, (1987), PP. 148-153.
- [3] Gupta T.C, "Identification and Experimental Validation of Damping Ratios of Different Human Body Segments through Anthropometric Vibratory Model in Standing Posture," Journal of Biomechanical Engineering, Vol. 129, No.

- 4, ASME, (2007), PP. 566-574.
- [4] Garg, P.D., Ross, A.M., "Vertical Mode Human Body Vibration Transmissibility," Journal of IEEE transaction on systems, man and cybernetics, Vol. SMC-6, No. 2, (1976), PP.102-112.
- [5] Chi, L., Qiu, Y., Griffin, M.J., "Dynamic forces over the interface between a seated human body and a rigid seat during vertical whole body vibration," Journal of Biodynamics, Vol. 61, (2017), PP. 176-182.
- [6] XuBai, X., XuXu, S., Cheng, W., Qian, L.J., "On 4-degree of freedom biodynamic models of seated occupants:Lumped Parameter modelling," Journal of Sound and Vibration, Vol. 204, (2017), PP. 122-141.
- [7] Kishore, N.V., Saran, V.H., Harsha, S. P., "Transmissibility and DPMI analysis of the seated Human under Low frequency vibration," (2009).
- [8] Fairley, T.E., and Griffin, M.J., "The Apparent mass of the seated human body: vertical vibration," Journal of Biomechanics, Vol. 22, No 2, (1989), PP. 81-94.
- [9] Wang, W., Rakhejaa, S., Boileau P.E., "Relationship between measured aPParent mass and seat-to-head transmissibility responses of seated occupants exposed to vertical vibration," Journal of Sound and Vibration, Vol. 314, (2008), PP. 907-922.
- [10] Mostafa, A.M., Abdeen, Abbas, W., "Analytic Investigation and Numeric Prediction for Biodynamic Response of the Seated Human Body" Journal of American Science, Vol. 6, (2010), PP. 228-239.
- [11] Deboli, R., Calvo, A., Preti, C., "Whole-Body Vibration: Measurement of Horizontal And Vertical Transmissibility of an Agricultural Tractor Seat," Int. Journal of Industrial Ergon., Vol. 58, (2017), PP. 69-78.
- [12] Liang, C.C., Chiang, C.F., "A study on biodynamic models of seated human subjects exposed to vertical vibration," International Journal of Industrial Ergonomics, Vol. 36, (2006), PP. 869-890.
- [13] Coyte, J.L., Stirling, D., "Seated Whole-Body Vibration Analysis, Technologies, and Modeling: A Survey," IEEE, (2015), PP. 2168-2216.
- [14] Mansfield, N.J., "Impedance Methods (APParent Mass, Driving Point Mechanical Impedance and Absorbed Power) for Assessment of the Biomechanical Response of the Seated Person to Whole-body Vibration," Industrial Health, Vol. 43, (2005), PP. 378-389.
- [15] Jamshidi, R., "Human-machine System Scheduling According to Fatigue and Learning Effects," International Journal of Industrial Engineering and Production Research, Vol. 27, No. 3, (2016), PP. 265-274.
- [16] Mehdizadeh, E., Fatehi-kivi A., "A Vibration Damping Optimization Algorithm for Solving the Single-item Capacitated Lot-sizing Problem with Fuzzy Parameters," International Journal of Industrial Engineering and Production Research, Vol. 28, No. 1, (2017), PP. 33-45.
- [17] Naeini, H,S, Dalal, K., Mosaddad, S, H., Karuppiah, K, "Economic Effectiveness of Ergonomics Interventions," International Journal of Industrial Engineering and Production Research, Vol. 29, No. 3, (2018), PP. 261-276.
- [18] Kociolek, A.M., Lang, A.E, "Exploring head and neck vibration exposure from quad bike use in agriculture," International Journal of Industrial Ergonomics, Vol. 66, (2018), PP. 63-69.

- [19] Boileau P.E., "A study of secondary suspensions and human drivers response to whole body vehicular vibration and shock," PhD. Thesis, Concordia university, (1995).
- [20] Grover G.K., "Mechanical Vibration," 7th Edition, Nem Chand & Bros. Roorkee, India, (2003).
- [21] Griffin, M.J., "Hand book of Human Vibration," Academic Press, London, (1990).
- [22] Nalavade, B., Bhortake, R.V., "Analysis of the Vibration Transmissibility of Automobile Seat Subject To Vertical Excitations," IJSART Vol. 2, No. 9, (2016), ISSN: 2395-1052.
- [23] Mechanical Vibration and Shock — Range of Idealized Values to Characterize Seated-Body Biodynamics Response under Vertical Vibration, International Organization for Standardization, (2001), IS/ISO 5982.
- [24] Nopiah, Z., Junoh, A., Muhamad, W.Z., "Linear Programming: Optimization of Noise and Vibration Model in Passenger Car Cabin," Vol.2 ,No.1. (2012), PP. 2251-7545.
- [25] Dragan, S., Vlastimir, D., "The Effect Of Stiffness And Damping of the Suspension System Elements on the Optimisation of the Vibrational Behaviour of a Bus," International Journal for Traffic and Transport Engineering, Vol. 1, No. 4, (2011), PP. 231 – 244.

Follow This Article at The Following Site:

Phate M, Gaikwad P. Exploring Biodynamic Response (Apparent Masses) of a Seated Human Body Exposed To External Excitation in Vertical Direction. IJIEPR. 2018; 29 (4) :415-428

URL: <http://ijiepr.iust.ac.ir/article-1-844-en.html>

